Journal of Science: Advanced Materials and Devices 8 (2023) 100543

Contents lists available at ScienceDirect

Journal of Science: Advanced Materials and Devices

journal homepage: www.elsevier.com/locate/jsamd

Original Article

Reproducible, self-healable polyurethane composite networks with high toughness, florescence and water-insensitivity

Xiyang Zeng [a, b, 1], Yong Yang [a, 1], Tao Chen [a], Tuck-Whye Wong [d], Junfeng Li [b], Guilong Yan [e, ***], Ruqing Bai [c, **], Li Wang [a, b, *]

[a] School of Big Health and Intelligent Engineering, Chengdu Medical College, Chengdu 610500, PR China
[b] College of Materials, Chemistry & Chemical Engineering, Chengdu University of Technology, Chengdu 610059, Sichuan, PR China
[c] State Key Laboratory of Mechanical Transmission, Chongqing University, 400044 Chongqing, PR China
[d] Advanced Membrane Technology Centre, Universiti Teknologi Malaysia, Johor 81310, Malaysia
[e] School of New Energy and Materials, State Key Laboratory of Oil and Gas Reservoir Geology and Exploitation, Southwest Petroleum University, Chengdu 610500, Sichuan, PR China

ARTICLE INFO

Article history:
Received 30 November 2022
Received in revised form
14 January 2023
Accepted 3 February 2023
Available online 8 February 2023

Keywords:
Self-healing capability
Reproducibility
Fluorescence
Polyurethane networks
Water-insensitivity

ABSTRACT

For self-healing polymers, the poor elastic properties and low self-healing efficiency have limited their applications, and smart polymer systems adaptable to the complex environment have become a hot topic. To address this issue, in this study, a series of polyurethane composite networks were developed, using poly (ϵ-caprolactone) (PCL) and polytetramethylene ether glycol (PTMG) as the soft segment, isophorone diisocyanate (IPDI) as the hard segment, with the incorporation of florescent $SrAl_2O_4$: Eu^{2+}, Dy^{3+} phosphors. The chemically crosslinked networks were investigated by differential scanning calorimetry (DSC), X-ray scattering (XRD), and dynamic mechanical analysis (DMA) on their crystalline properties. Atomic force microscopy (AFM) confirmed the micro-phase separation structures, where soft segments facilitated self-healing and the hard segments enhanced rigidity. Scanning electron microscopy (SEM) and optical microscopy presented highly efficient and rapid healing could be achieved. The materials emitted an intense green light in UV without significant fluorescent intensity reduction in water emersion. Additionally, the synergistic effect of transesterification provided the composite networks reproducibility for recycling use.

1. Introduction

Smart materials are a kind of material that can sense the environment or its own state, and change their function according to a predetermined purpose by making a judgment [1,2]. Most conventional smart materials are not recyclable and sustainable, and physical damage can cause chains to crack and slip, leading to further damage to the material [3]. Even if the material is undamaged, prolonged use can lead to deterioration and waste, which is uneconomical and environmentally friendly [4]. Self-healing polymers can effectively repair mechanical damage, generating interest from a wide range of researchers [5,6]. The healing mechanism of self-healing polymers is divided into extrinsic and intrinsic. Intrinsic self-healing has superior repair capacity and sustainable potential for use compared to extrinsic self-healing [7]. Intrinsic self-healing assumes many forms, such as hydrogen bond, host–guest interaction, metal–ligand coordination, ionic interaction, π-π stacking, and disulfide bond [4,8–11]. So far, the healing processes of most self-healing materials require stimulation by external conditions, such as light [12], heat [13], and magnetism [14]. These self-healing materials with excellent properties provide the matrix with structurally tunable, superior performance, and thus could be used in a wide range of applications in biomedicine [15,16], sensors [17], wearable electronics [18], and aerospace [19].

* Corresponding author. School of Big Health and Intelligent Engineering, Chengdu Medical College, Chengdu 610500, PR China.
** Corresponding author.
*** Corresponding author. School of New Energy and Materials, State Key Laboratory of Oil and Gas Reservoir Geology and Exploitation, Southwest Petroleum University, Chengdu 610500, Sichuan, PR China.
E-mail addresses: guilong.yan@swpu.edu.cn (G. Yan), ruqing.bai@cqu.edu.cn (R. Bai), liwang@cmc.edu.cn (L. Wang).
Peer review under responsibility of Vietnam National University, Hanoi.
[1] Authors contributed euqally.

https://doi.org/10.1016/j.jsamd.2023.100543

The mobility of the chain segments contributes to the surface proximity of molecular chain damage and interdiffusion, which is the basis for self-healing polymers to heal based on dynamic chemical bonding [20]. Although the good mobility of the chain segments allows self-healing polymers to heal themselves well, it can lead to poor mechanical properties [21,22]. To resolve the conflict between mechanical properties and self-healing effects, microphase separation of polyester-based polyurethanes (PUs) provides a rational approach, with the hard segments providing the strength of the material and the soft segments providing the mobility of the chain segments, thus contributing to the self-healing of materials with high mechanical properties [23,24]. Semi-crystalized poly (ϵ-caprolactone) (PCL) based PUs could present a transition temperature for chain movements above melting transition, while their rigid crystalized phases could provide the materials with excellent mechanical properties at room temperature. On the other hand, polytetrahydrofuran (PTMG) with a flexible polymer chain structure facilitates the mobility of the polymer chains at ambient temperature. In recent years, many researchers utiliized PTMG as a soft segment structure to ensure good mobility of the chain segments for self-healing properties [25]. For PU network formation, isophorone diisocyanate (IPDI) with an asymmetric alicyclic structure could provide PU with sufficient chain segment mobility compared with other cross-linkers. Jia and his colleagues prepared polyurethanes using PEG and IPDI, which have excellent self-healing properties and elongation at break of 2800% and 93%, respectively, but with a fracture strength of only 1.05 MPa [26]. Lee and his co-workers prepared polyurethane prepolymers using PTEMG, DMPA and IPDI, with chitosan as a chain extender. Its tensile strength was up to 33.6 MPa. However, its self-healing efficiency after heat treatment at 110 °C for 24 h was only 47% [27]. By the reaction of PCL, PTMG, and IPDI, PU maintained its high self-healing efficiency, and two microscopic phase separation domains could enhance PU with high mechanical properties. Moreover, strontium aluminate phosphors could further enhance the mechanical properties of PU, while providing higher brightness and persistent glow time than traditional sulphide phosphors [28,29]. Therefore, after the incorporation of rare earth luminescent materials of $SrAl_2O_4$ doped by Eu^{2+} and Dy^{3+} (SAED), a pre-determined pattern under the irradiation of ultraviolet (UV), temporary information could be presented and erased with the healing process.

In this study, a crosslinked elastic polyurethane network with self-healing capability and recyclability was developed. The soft segment of polyurethane was composed of semi-crystalized poly (ϵ-caprolactone) (PCL) and polytetrahydrofuran diol (PTMG), and the isophorone diisocyanate (IPDI) was chosen to be the hard segment (Fig. 1a), its healing capacity was provided mainly by the reorganization of hydrogen bonds (Fig. 1b). In addition, $SrAl_2O_4$ doped by Eu^{2+} and Dy^{3+} (SAED) was added as filler, stimulating UV triggered fluorescent effect (Fig. 1c). Systematic characterization of their physical and chemical properties, micro-morphologies were accessed. The self-healing properties of the composite films were evaluated by stretching and the microphase separation structure was observed by AFM. By observation by SEM, and optical microscopy, the self-healing effect was analyzed. After intense green light under a 365 nm UV lamp was performed on the networks to show the fluorescent effect and self-healing process. Finally, the recyclability of the materials was evaluated by process into different shapes.

2. Experimental

2.1. Materials

Polycaprolactone diol (PCL, M_n = 4000 g/mol) and polytetramethylene ether glycol (PTMG, M_n = 4000 g/mol) were purchased from Jining Hua Kai Resin Co., Ltd. Tin 2-ethylhexanoate ($C_{16}H_{30}O_4Sn$, >95.0%) and isophorone isocyanate (IPDI, $C_{12}H_{18}N_2O_2$, >99.0%) were purchased from Aladdin Chemical Reagent Factory. $SrAl_2O_4$ doped by Eu^{2+} and Dy^{3+} (SAED) was obtained from Honest Technology Luminous Material Development Co., Ltd.

2.2. Synthesis of PU and SEAD/PU composite films

Preparation of self-healing PU films: PCL and PTMG (3:7–7:3) were completely melted and stirred well in an oil bath at 80 °C under a nitrogen atmosphere at 100 r/min. 3 ml of IPDI and drops of tin 2-ethylhexanoate were added to the viscous solution and reacted for 4 h. The viscous react mixture was then transferred to a polytetrafluoroethylene mold and cured in an oven at 100 °C for 12 h. The film was finally obtained by cooling and demolding at room temperature. The crosslinked network films were named PUx (x stands for the ratio of PCL content in PU as x*10 wt%). SAED/PU

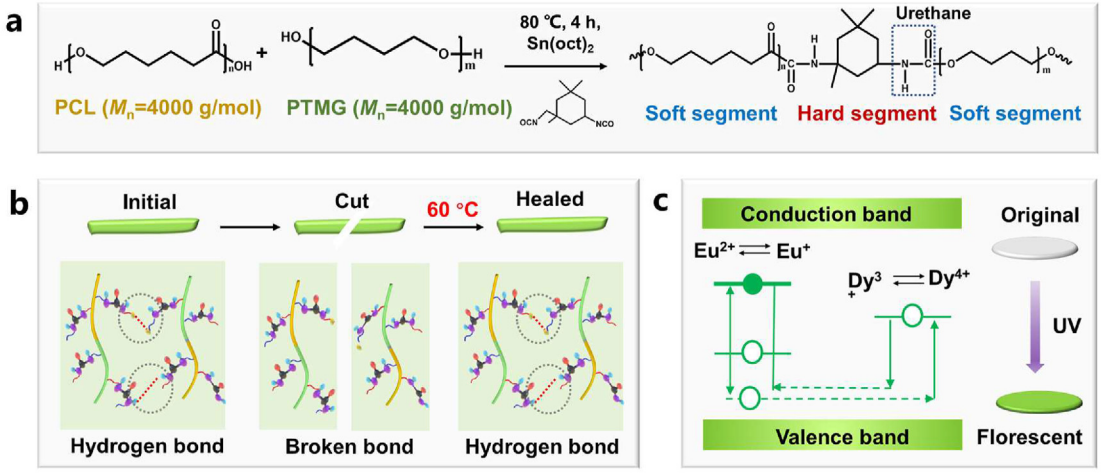

Fig. 1. (a) Synthesis route of cross-linked polyurethane networks. (b) Self-healing mechanism of polyurethane network films. (c) Luminescence mechanism of composite network films.

composite films were synthesized by in situ polymerisation as described above, with the difference that $SrAl_2O_4$ particles (5–20 wt%) were added before IPDI and 2-ethylhexanoate, and stirred for 10 min after complete addition.

2.3. Materials characterization

Mechanical tensile properties and self-healing efficiency tests: The tests were carried out using an electronic universal testing machine, model MIT-30KN, from Changzhou SFMIT Instruments Co. Tensile experiments on five different scales of composite films were carried out under natural environmental conditions with samples of 30 mm length ×10 mm width × 2 mm thickness and a stretching rate of 5 mm/min, 65% RH. Each set of samples was tested at least three times. For the self-healing test, the composite film was cut into two pieces and then the cut surfaces were contact healed at 60 °C. The healed composite film was then subjected to a tensile test to measure the healing efficiency (the ratio of elongation at the break between the healed film and the original film). The storage modulus, loss modulus, and internal consumption of network films were measured using a Q800 Dynamic Mechanical Analyzer (TA, USA). At a dynamic strain of 0.1% and a constant frequency of 1 Hz, the temperature range was from −100 to 60 °C and the heating rate was 5 °C/min.

The weight of the film was recorded (M_1) after it was cut into small pieces 10 mm in length, 10 mm in width and approximately 2 mm in thickness. The film was soaked in ethyl acetate solution for 24 h and then removed. The weight of the film was recorded (M_2) on filter paper after absorbing the solution from the surface of the film. Finally, the film was dried in an oven at 60 °C for 12 h and recorded the weight (M_3). The average value was measured by repeating three times and the gel content (G) and swelling rate (S) were calculated as follows: $G\,(\%) = M_3/M_1 \times 100\%$, $Q\,(\%) = M_2/M_1 \times 100\%$.

The functional groups of network films were analyzed in the wavelength range 400–4000 cm^{-1} using a Fourier Transform Infrared Spectrometer (FTIR, TENSOR-27, Bruker, Germany) with 64 scans of each spectrum and a resolution of 4 cm^{-1}. At room temperature, the water contact angle of network films (10 × 10 × 2 mm) was determined by a contact angle meter (SDC 200, Dongguan Yuding Precision Instrument Co., Ltd.), and the average value was taken three times. The melt temperature trend of the films was observed using differential scanning calorimetry (DSC, NETZSCH DSC-204F1) to measure thermal changes. All operations were carried out under a nitrogen atmosphere. In this case, the heating and

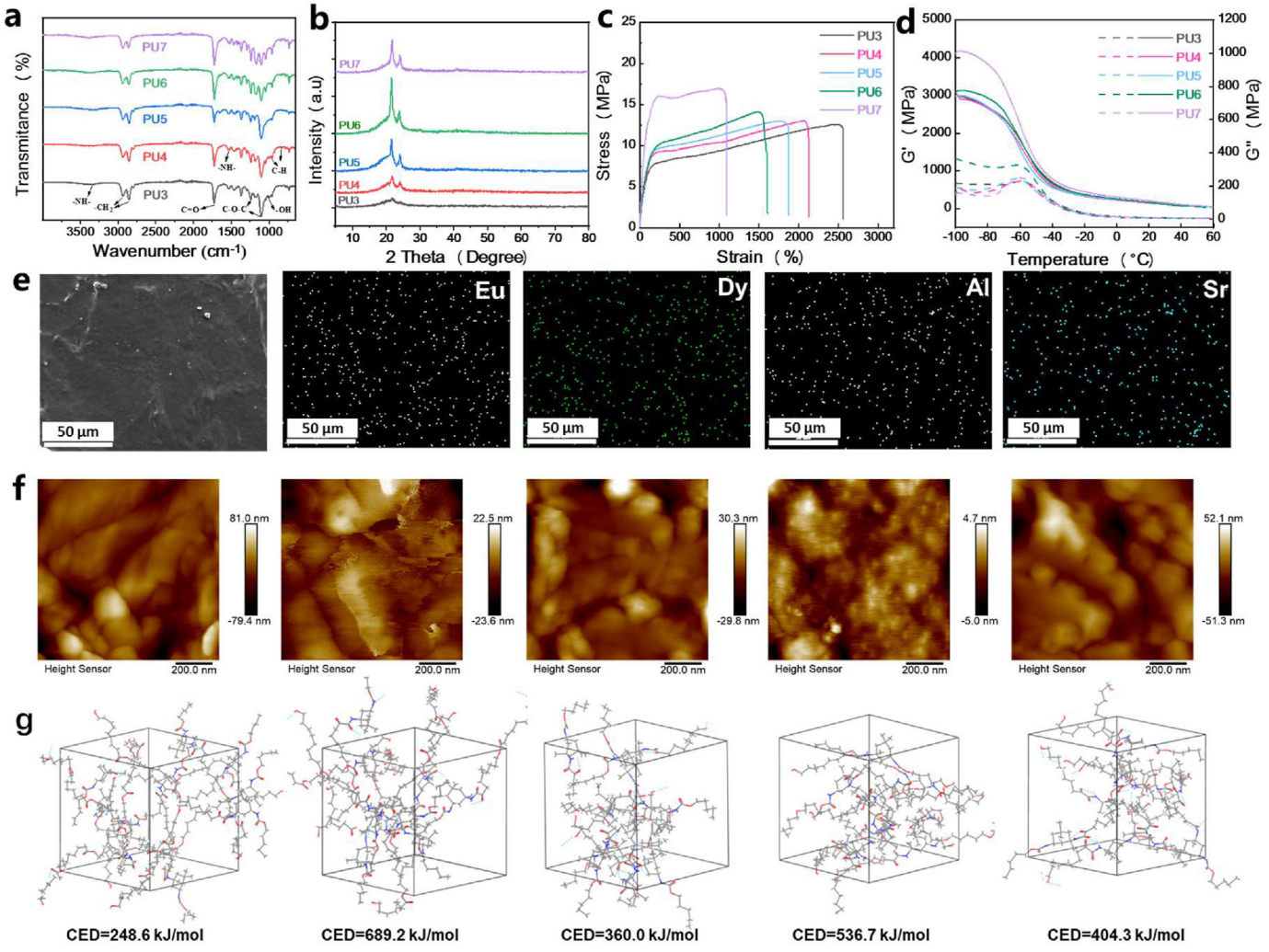

Fig. 2. (a) Infrared spectra of PU network films. (b) XRD spectra of network films. (c) Stress–strain curve for network films from tensile test. (d) Variation of storage modulus (G′) and loss modulus (G″) of network films with temperature. (e) EDS particle diagram for network composite films. (f) AFM images of network composite films. (g) A Snapshot of an all-atom MD simulation of a network composite film with different ratios of PCL/PTMG from 3:7 to 7:3, the bat model emphasizes the hard part.

cooling rates were both 10 °C/min. The sample was heated from room temperature to 100 °C and maintained for 3 min to eliminate the thermal history. It was then cooled from 100 °C to −50 °C and finally, a second scan was conducted from −50 °C to 100 °C. The thermal stability and fluorescence powder content of the composite films were determined by thermogravimetric analysis (TGA, NETZSCH, STA449F3, Germany). The scanning range was from room temperature to 800 °C with a heating rate of 10 °C/min.

The self-healing process of the composite film was analyzed using field emission scanning electron microscopy (FE-SEM, INSPECTF50, FEI, Holland) at an accelerating voltage of 10 kV. The dispersion of the phosphor in the composite film was also observed using energy dispersive spectroscopy (EDS). The composite film was cut into small pieces of 5 × 5 × 2 mm, and the surface morphology of the network films was observed on atomic force microscopy (AFM, Brucker Icon) with a tapping method. Four composite films of different proportions (5–20 wt%) were prepared in 10 × 10 × 1 mm blocks and PL emission spectra were recorded on a fluorometer (F4600, Japan) with an excitation wavelength of 518 nm.

3. Results and discussion

3.1. Characterization of PU films

Detailed information about the material properties, i.e., crystalline properties, water contact angle, degree of swelling, and gel content of the network materials was provided in the supporting information (Figs. S1–S4, Tables S1–S2). Fig. 2a showed the FTIR spectrum of the PU films with a carbamate C═O stretching vibration peak at 1725 cm^{-1}, indicating the formation of a covalent crosslinking network. The absence of the characteristic peak for the −N═C═O group at 2300 cm^{-1} indicated that the IPDI reacted completely. The FTIR results confirmed the successful preparation of self-healing polyurethane films. The gel content of the network film decreased as the PTMG content increased, due to the movable PTMG chains helped the crosslinking of the films, the overall values of gel content were all above 85% (Fig. S1), indicating the formation of fully crosslinked network structure. At the same time, the increase in PCL content restricted the movement of the chain segments, resulting in a decrease in the swelling of the film from 210% to 133% (Fig. S2). The contact angle of the network film increased from 87° to 98° as the PTMG content increased (Fig. S3). Fig. 2b showed that the crystalline peak intensity decreased with increasing PTMG content. This could be attributed to the fact that the increasing amount of PTMG hinders the regularity of the molecular chains, at the same time, more hydrogen bonds were formed within the PTMG molecules, which led to a lower melting temperature of PTMG. More details on the thermal properties of network films were presented in the supporting information (Fig. S4 and Table S1).

The mechanical properties of PU network films were investigated by tensile tests, as shown in Fig. 2c. In the stress–strain curve, the network films showed an initial strengthening region due to the crystalline of PCL at room temperatures, and the presence of dynamic H-bonds between the chains enhanced the elasticity, followed by a stable region until a fracture occurs. The PU3 network film shows the highest elongation at break (2500%), the tensile strength and Young's modulus are 12.4 MPa and 7.9 MPa, respectively. In addition, the Young's modulus, tensile strength, elongation at break, and fracture energy of network films with different

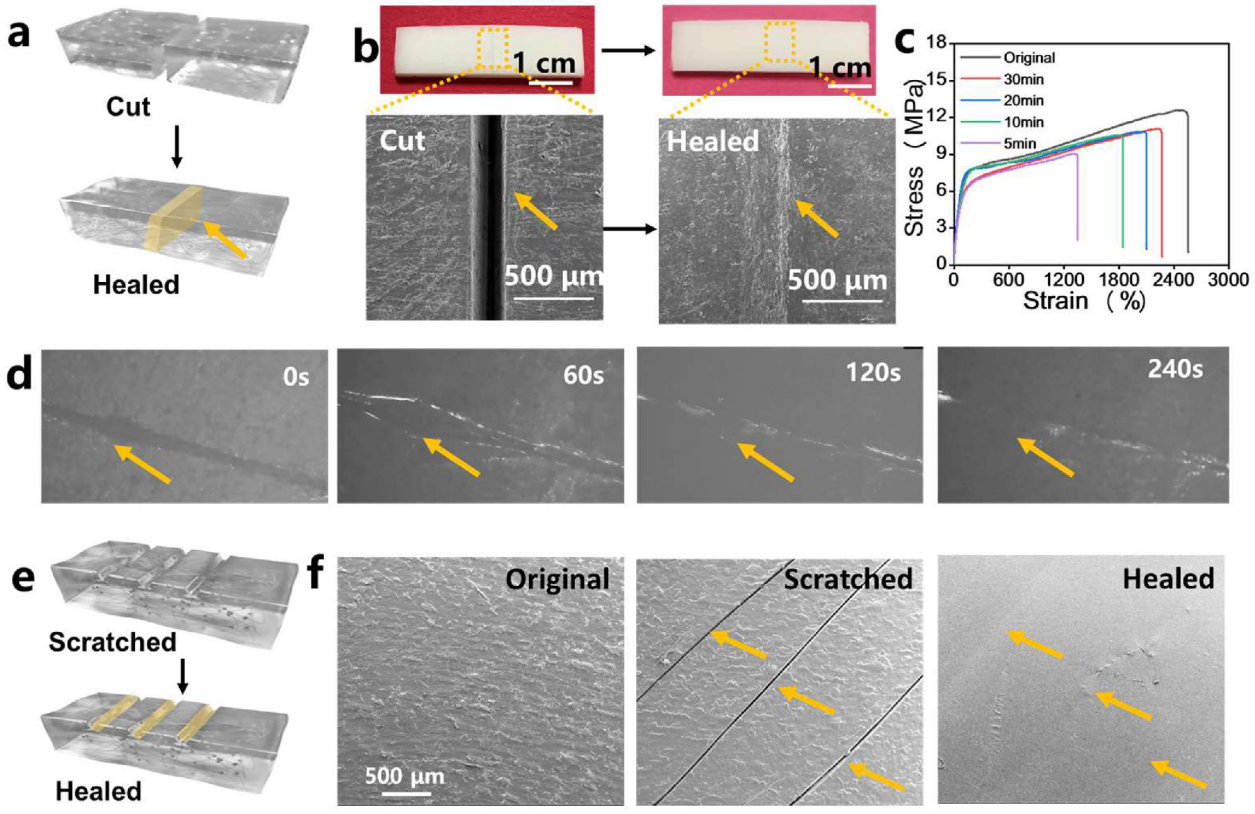

Fig. 3. (a) Diagram of network film healing process after the cut. (b) Physical photo of the network film after cutting and healing, and SEM image of the corresponding cut and healed area. (c) Stress–strain curves of cross-linked networks at different healing times. (d) Healing diagram of network film at different times under a light microscope. (e) Diagram of scratch healing of network film. (f) SEM images of the network composite film from areas of original undamaged, after scratching, and healed places at 60 °C.

PCL/PTMG ratios were described in detail in the supplementary information (Figs. S5–S9 and Table S2). As the PCL content increased, the elongation at the break of the film gradually decreased while the tensile strength raised, mainly because the increase in PCL limited the ability of the polymer chains to move or caused stress concentration. In addition, the elongation at break was significantly reduced due to the high density of hydrogen bonding crosslinks.

To further illustrate the chain mobility and viscoelastic behavior of the network composite film, the temperature dependence of the storage modulus (G′) and loss modulus (G″) was characterized by dynamic mechanical analysis. As shown in Fig. 2d, G' was consistently higher than G″, indicating that the PU films were in a solid state. The PU7 film exhibited the highest storage modulus due to its more intensive hydrogen bonding cross-linking. At around −70 °C, the modulus tended to decrease, indicating the onset of soft segment movement. As the temperature rises above −60 °C, the modulus of all networks dropped sharply, which means that the hydrogen bonds begin to dissociate. As the temperature raised to 60 °C, the sample film turned softened. They could not retain their shape due to the dissociation of most of the intermolecular hydrogen bonds, and all composite films began to be in a liquid state after higher than 60 °C. The glass transition temperature of the network film was around −46 °C, indicating its highly elastic state at room temperature. The glass transition temperature of the composite film decreases significantly with increasing PCL content. Furthermore, to verify the elemental composition of the phosphor, the distribution of all elements (Sr, Al, Eu, Dy) was characterized using EDS analysis. As could be seen from the EDS plots in Fig. 2e, the uniform distribution of these elements indicated trace doping, and all elements were uniformly dispersed in the composite film, indicating good dispersion of the SAED powder among the PU matrix.

The AFM images in Fig. 2f showed that the network films had a microphase separation structure consisting of soft segments (PTMG and PCL, dark region) and hard segments (H-bonded aggregates, bright region) agglomerated. All samples exhibited a clear microphase separation, with increasing PTMG content, a more pronounced microphase domain size appeared due to the rising hydrogen bonding interactions. Therefore, the increase of PTMG not only promoted the formation of strong hydrogen bonds but also promoted microphase separation, which finally improved the mechanical properties of the material and resolved the conflict between mechanical strength and self-healing ability.

Fig. 2g exihibited molecular dynamic simulation (MD) results with the PCL/PTMG ratios of 5:5, 6:4, 4:6, 7:3, 3:7. Herein, the cohesive energy densities (CED) were calculated by COMPASS. All models showed CED values over 200 kJ/mol. Especially, when the PCL/PTMG ratios were 6:4 and 7:3, the CED values were larger than others, which meaned higher van der Waals force in a PU network unit and better mechanical properties. The MD results were consistent with the experimental results.

3.2. Self-healing efficiency of network composite films

In this study, self-healing polyurethanes were developed, in which dynamic urethane bonding and hydrogen bonding provided the network films the ability with a self-healable effect. Further characterizations of its healing performance tensile tests and

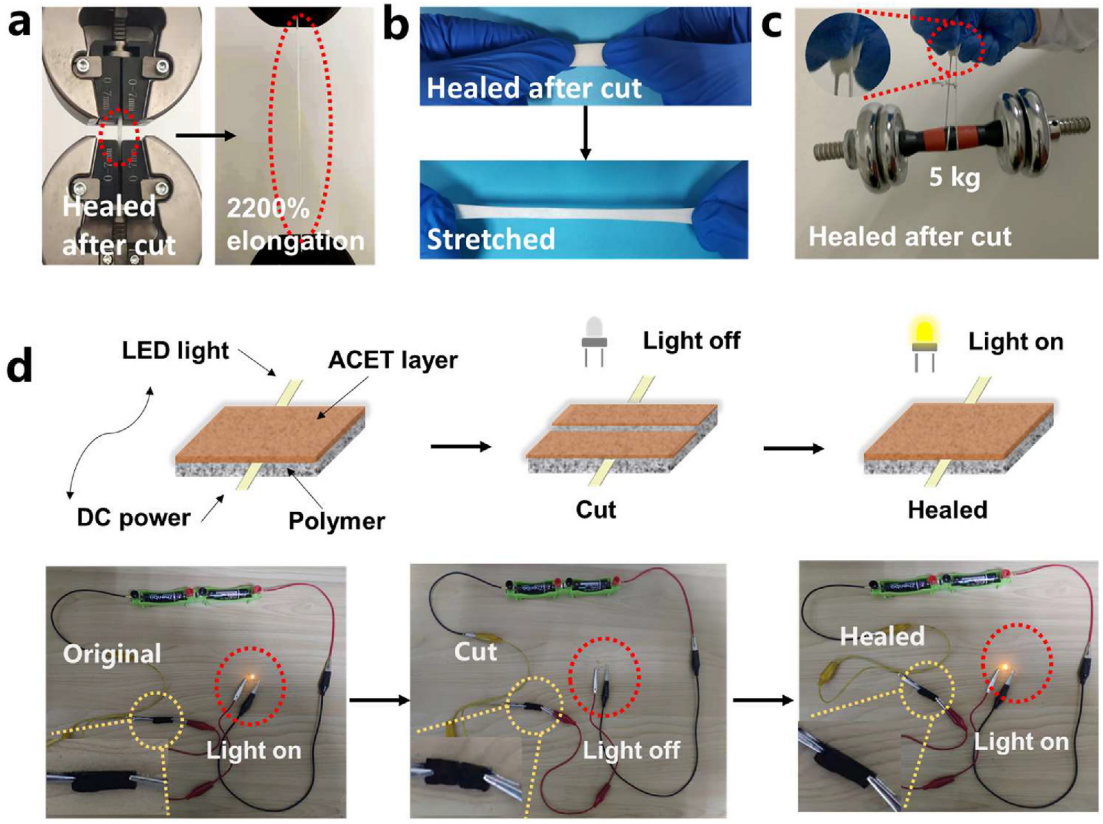

Fig. 4. (a) Photograph of PU network sample stretch to over 2200% after healing. (b) Stretching of healed PU film sample by human hands. (c) Images of healed PU film sample by lifting 5 kg dumbbell. (d) Schematic illustrating a simple electronic circuit and composite conductor preparation. The LED was illuminated during the original phase and switched off during the conductor severing phase. At 60 °C, the severed composite conductor heals effectively after 5 min and the LED was illuminated.

microscopic measurements were carried out on PU5. As shown in Fig. 3a and b, a small incision was made in the middle of the network film, and kept at 60 °C for half an hour, as a result, the film notch was completely healed after heating. To assess the self-healing ability of the PU film at different temperatures, the stress–strain curves before and after healing were performed and the self-healing efficiency of the network sample was calculated. As shown in Fig. 3c, the network was healed at 60 °C for 5, 10, 20, and 30 min respectively for the tensile curve. Elongation at break increased from 1349% to 2272% when the healing time increased from 10 min to 30 min, self-healing efficiency increased significantly from 52.8% to 88.8% (Figs. S10–15). Fig. 3d showed the healing process of the network film under the light microscope. A cut was firstly made on the sample, then it was heated to 60 °C, the sample turned viscous after the 60 s and started to heal. After 240 s the cut on the sample was completely healed (Fig. 3d, Video S1). Another scratch experiment was performed on this sample, as shown in Fig. 3e and f. No scratches were found on the original sample, and by an external force, three scratches were made on the surface of the network film. After healing at 60 °C, the SEM images showed that the scratches on the surface of the network film almost disappeared and the surface became smooth without any obvious scratches.

To demonstrate the self-healing efficiency of PU film, tensile tests were done and as could be seen in Fig. 4a. After healing, the samples were elongated by the tensile test machine, and the elongation of the films after healing could reach 2200%. In addition, the network maintained its excellent elasticity and toughness, by showing stretching with human hands, as shown in Fig. 4b. In Fig. 4c, after healing the network film could be used for lifting a 5 kg dumbbell. Interestingly, after 5 repetitions of the cut-and-heal experiment, it was still able to carry 5 kg dumbbells well. To demonstrate the self-

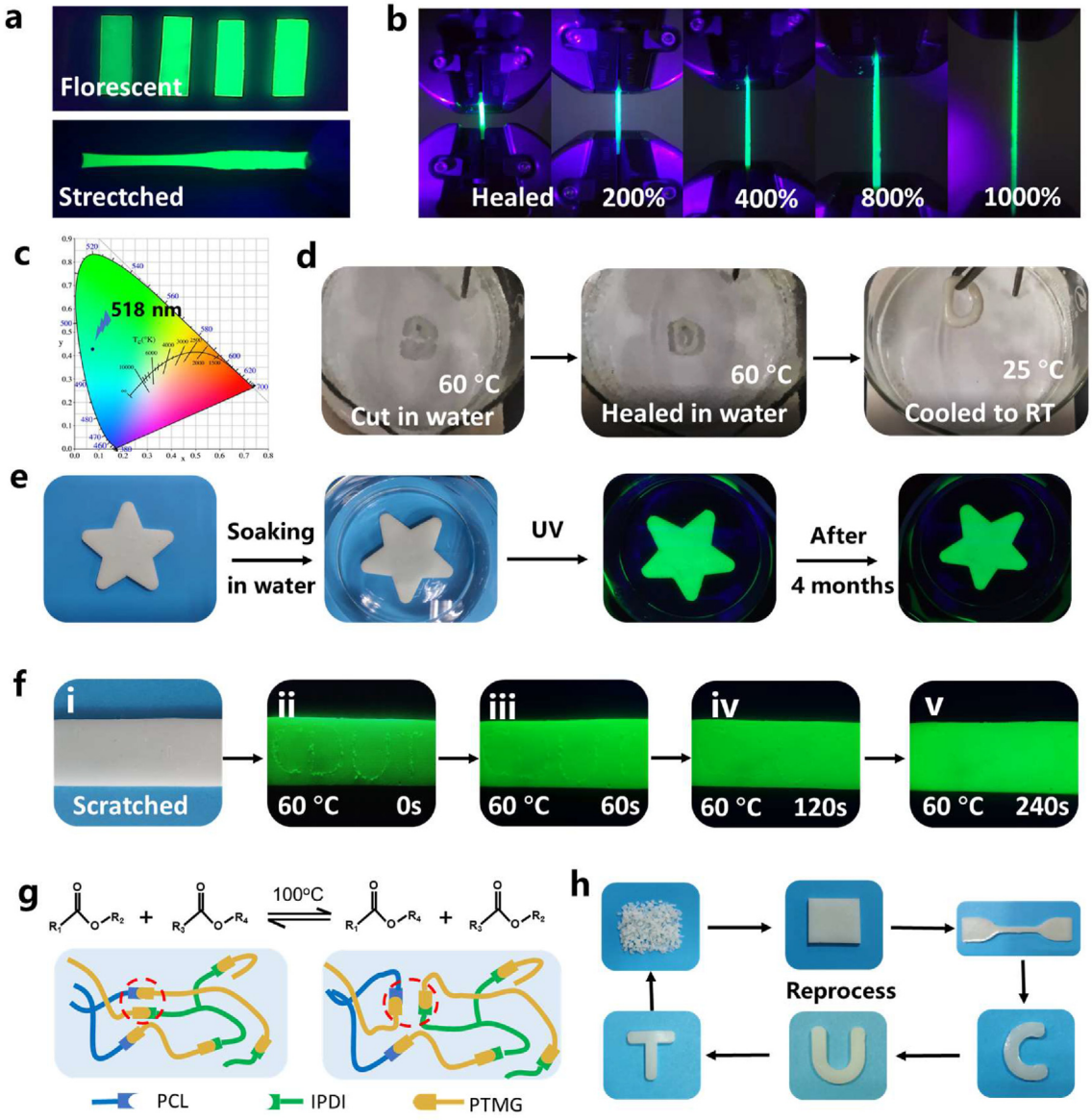

Fig. 5. (a) Luminescence and stretching of network composite films with different SAED content under 365 nm UV lamp. (b) Fluorescence images of SAED/PU composite network film before and after stretching excited by a 365 nm UV lamp. (c) CIE color coordinates for network composite films. (d) Self-healing ability of PU film in an aqueous environment. (e) Photographs of SAED/PU film in natural light and UV light, and after 4 months of immersion in water. (f) The anti-counterfeiting function of the films by showing CDUT scratches and its fluorescent effect before and after healing. (g) Reprocess and reshape mechanism of SAED/PU samples, and (h) the composite network films were cut into small pieces and then reprocessed by hot pressing method.

healing capability, an electric lamp system was used to present the healing effect of polymer cut, by surface coating an electrically conductive layer, as shown in Fig. 4d. Specifically, acetylene black (ACET) was dissolved in a small amount of alcohol and ground to a viscous state. Successively the acetylene black solution was evenly applied to a PU network film, which was constructed as a stretchable and self-healing conductor. With this conductor and a 3 V voltage battery a circuit effectively was illuminated with a connected light emitting diode (LED) lamp. When the composite conductor was cut into two pieces, the LED was off as no electricity through the current. After heating at 60 °C for 5 min, the two cut pieces could heal themselves and the LED was illuminated again, depending mainly on the re-formation of hydrogen bonds (Fig. 4d). This was much faster than the healing rate of some self-healing conductors reported so far, which take several hours to heal.

3.3. Fluorescence and recycling property of SAED/PU network films

Under UV light (365 nm), the white fluorescent SAED powder could show an intense green luminescence. The excitation spectrum of the SAED phosphor obtained from the 365 nm emission peak was obtained using a fluorometer (Fig. S16), while the emission spectrum of the phosphor excited at 518 nm was given (Fig. S17). It is worth noting that, as shown in Fig. 5a, after embedding SAED into the PU matrix, the composite films could emit green light under UV light (365 nm), while the luminescence intensity increased with the increase of SAED content. The composite films could maintain bright green light when stretched, which could almost recover their original shape after release, showing excellent flexibility and fluorescence effect. In addition, by the tensile test machine, the composite network film could present green light even stretched to 1000% as shown in Fig. 5b. Furthermore, Fig. 5c showed the CIE position of the fluorescence emission at 518 nm excitation, which was located at (0.0755, 0.4268). The excitation spectrum of the composite network film obtained from the 365 nm emission peak was shown in Figs. S18 and S19. The excitation peak was significantly enhanced between 300 and 400 nm, which was mainly due to the increase of the rare earth strontium aluminate content and the Eu^{2+} content in the luminescence center. The main influencing factor of the luminescence performance of the composite film was Eu^{2+}, the electronic layer of the rare earth ion Eu^{2+} was scattered with a variety of energy levels of sub-stable energy states, the different energy levels of sub-stable energy states can absorb the light stored at different wavelengths, when irradiated with excitation light, the rare earth ion Eu^{2+} absorbs light energy, the outer layer of Eu^{2+} electrons jump between different energy levels of the ground state, sub-stable energy states, and excited states, resulting in a variety of absorption bands, which form a continuous absorption spectrum. The emission spectrum of the composite network film excited at 518 nm, the position of the emission peak did not change significantly, but the intensity of the emission peak at 518 nm increased with the increase of SAED content.

The self-healing of SAED/PU films was water insensitive, as shown in (Fig. 5d), after cutting in water at 60 °C, the sample could heal itself as in a nonaqueous environment in 5 min. The florescent resistance of the composite network film to water was studied by immersing it in water. As the experimental results shown in Fig. 5e, the SAED/PU film presented an intense green light after 4 months of immersion in water. It suggested that the composite network film had a high degree of long-term stability in fluorescence without significant fading and degradation.

To demonstrate the anti-counterfeiting function of the films obtained by combining phosphors with PU, the film was marked with the letters “CDUT”. Under natural light, these marks were barely recognizable to the human naked eyes, however, they emitted green color of light under UV light, and scratched in the shape of “CDUT” appear on the surface of the various films, which gradually diminish as the self-healing process deepens, taking only 15 min before the scratches were completely invisible (Fig. 5f). On the other hand, the composite network films showed white color in sunlight, but emitted a green light under UV light, making them tamper-proof. This visible-light invisible and UV-visible polyurethane presented attractive potential as an anti-counterfeiting ink or coating. The unique fluorescent properties and flexibility of network film made it a promising anti-counterfeiting ink.

Moreover, the composite network exhibited excellent plasticity and reproducibility at high temperatures. As shown in Fig. 5g and h, network film was cut into small pieces and left at 100 °C for 2 h while pressurizing, and remolding the composite film with its flexibility, the samples could be reprocessed into different shapes. This was mainly attributed to the reconfiguration of the network by dynamic urethane bond exchange reactions at high temperatures, and the progressive increase in the probability of urethane bond transformation with increasing contact time, to realize polyurethane remodeling [30]. In addition, the characteristic peaks of the IR spectra of the polyurethane material with the addition of 5% white fluorescent SAED powder did not change significantly before and after remolding, indicating no change in its chemical structure (Fig. S20). At the same time, the mechanical properties of the remolded SAED/PU samples were slightly reduced, all of which proved the good recyclability of the material (Fig. S21).

4. Conclusion

In summary, we have designed a range of polyurethane films with a fluorescent effect that combines self-healing capabilities with high toughness. The films were composed of semi-crystalized PCL and elastic PTMG as the soft segment, isophorone diisocyanate (IPDI) as the hard segment, with the incorporation of florescent $SrAl_2O_4$: Eu^{2+}, Dy^{3+} (SAED) phosphors. From the results, the network materials were confirmed with micro-phase separation structures, where soft segments facilitated self-healing and the hard segments enhanced rigidity. From the SEM and optical microscopy images, the self-healing materials presented highly efficient and rapid healing effect. Additionally, the materials showed a fluorescent effect, which emitted an intense green light in UV with no significant fluorescent intensity reduction in water emersion. Finally, the materials showed reproducibility for recycling use due to the transesterification. The obtained self-healing network materials could be a promising candidate in applications of smart, robust applications.

Declaration of competing interest

The authors declare that they have no known competing financial interests or personal relationships that could have appeared to influence the work reported in this paper.

Acknowledgment

This research was funded by Sichuan Science and Technology Program [2021YFH0098], China Postdoctoral Science Foundation [2022M710514] and the Joint Scientific Research Fund of Chengdu Medical College - People’ Hospital of Chengdu Pidu District [202lLHPJ-03].

Appendix A. Supplementary data

Supplementary data to this article can be found online at https://doi.org/10.1016/j.jsamd.2023.100543.

References

[1] D. Mukherji, C.M. Marques, K. Kremer, Smart responsive polymers: fundamentals and design principles, Ann. Rev. Con. Mat. Phy. 11 (2020) 217–299.
[2] L. Tang, L. Wang, X. Yang, Y.Y. Fen, Y. Li, W. Feng, Poly(N-isopropylacrylamide)-based smart hydrogels: design, properties and applications, Prog. Mater. Sci. 115 (2021) 53.
[3] D.B. Guillaume, Combining mobile and dynamic bonds for rapid and efficient self-healing materials, Chem 5 (2016) 668–673.
[4] W.J. Lee, H.G. Oh, S.H. Cha, A brief review of self-healing polyurethane based on dynamic chemistry, Macromol. Res. 29 (2021) 649–664.
[5] W.J. Yao, Q.Y. Tian, J.Q. Shi, C.S. Luo, W. Wu, Printable, down/up-conversion triple-mode fluorescence responsive and colorless self-healing elastomers with superior toughness, Adv. Funct. Mater. 31 (2021) 11.
[6] G. Thangavel, M.W.M. Tan, P.S. Lee, Advances in self-healing supramolecular soft materials and nanocomposites, Nano Converg 6 (2019) 18.
[7] J.F. Patrick, M.J. Robb, N.R. Sottos, J.S. Moore, S.R. White, Polymers with autonomous life-cycle control, Nature 540 (2016) 363–370.
[8] S.M. Kim, H. Jeon, S.H. Shin, S.A. Park, J. Jegal, S.Y. Hwang, et al., Superior toughness and fast self-healing at room temperature engineered by transparent elastomers, Adv. Mater. 30 (2018) 8.
[9] Z.Q. Li, Y.L. Zhu, W.W. Niu, X. Yang, Z.Y. Jiang, Z.Y. Lu, et al., Healable and recyclable elastomers with record-high mechanical robustness, unprecedented crack tolerance, and superhigh elastic restorability, Adv. Mater. 33 (2021) 11.
[10] C.H. Li, J.L. Zuo, Self-healing polymers based on coordination bonds, Adv. Mater. 32 (2020) 29.
[11] X.H. Chen, X.Y. Zeng, K. Luo, T. Chen, T. Zhang, G.L. Yan, L. Wang, A multiple remotely controlled platform from recyclable polyurethane composite network with shape-memory effect and self-healing ability, Small 18 (2022), 2205286.
[12] H.C. Qian, D.K. Xu, C.W. Du, D.W. Zhang, X.G. Li, L.Y. Huang, et al., Dual-action smart coatings with a self-healing superhydrophobic surface and anti-corrosion properties, J. Mater. Chem. 5 (2017) 2355–2364.
[13] Y.L. Fang, X.S. Du, Z.L. Du, H.B. Wang, X. Cheng, Light- and heat-triggered polyurethane based on dihydroxyl anthracene derivatives for self-healing applications, J. Mater. Chem. 5 (2017) 8010–8017.
[14] A.S. Ahmed, R.V. Ramanujan, Magnetic field triggered multicycle damage sensing and self healing, Sci. Rep. 5 (2015) 10.
[15] M. Li, J. Chen, M.T. Shi, H.L. Zhang, P.X. Ma, B.L. Guo, Electroactive anti-oxidant polyurethane elastomers with shape memory property as non-adherent wound dressing to enhance wound healing, Chem. Eng. J. 375 (2019) 14.
[16] L. Wang, X.Y. Zeng, G.L. Yan, X.H. Chen, K. Luo, S.Y. Zhou, et al., Biomimetic scaffolds with programmable pore structures for minimum invasive bone repair, Nanoscale 13 (2021) 16680–16689.
[17] K. Kim, J. Park, J.H. Suh, M. Kim, Y. Jeong, I. Park, 3D printing of multiaxial force sensors using carbon nanotube (CNT)/thermoplastic polyurethane (TPU) filaments, Sens. Actuator A-Phys. 263 (2017) 493–500.
[18] Z.L. He, G.H. Zhou, J.H. Byun, S.K. Lee, M.K. Um, B. Park, et al., Highly stretchable multi-walled carbon nanotube/thermoplastic polyurethane composite fibers for ultrasensitive, wearable strain sensors, Nanoscale 11 (2019) 5884–5890.
[19] Y.B. Cai, H.W. Zou, S.T. Zhou, Y. Chen, M. Liang, Room-temperature self-healing ablative composites via dynamic covalent bonds for high-performance applications, ACS Appl. Polym. Mater. 2 (2020) 3977–3987.
[20] M.X. Liu, S. Zhu, Y.J. Huang, Z.H. Lin, W.P. Liu, L.L. Yang, et al., A self-healing composite actuator for multifunctional soft robot via photo-welding, Compos. B Eng. 214 (2021) 8.
[21] W.P. Chen, D.Z. Hao, W.J. Hao, X.L. Guo, L. Jiang, Hydrogel with ultrafast self-healing property both in air and underwater, ACS Appl. Mater. Interfaces 10 (2018) 1258–1265.
[22] L. Zhang, J.T. Wu, N. Sun, X.M. Zhang, L. Jiang, A novel self-healing poly(amic acid) ammonium salt hydrogel with temperature-responsivity and robust mechanical properties, J. Mater. Chem. 2 (2014) 7666–7668.
[23] H.G. Gui, G.W. Guan, T. Zhang, Q.P. Guo, Microphase-separated, Hierarchical macroporous polyurethane from a nonaqueous emulsion-templated reactive block copolymer, Chem. Eng. J. 365 (2019) 369–377.
[24] H.S. Guo, Y. Han, W.Q. Zhao, J. Yang, L. Zhang, Universally autonomous self-healing elastomer with high stretchability, Nat. Commun. 11 (2020) 9.
[25] J.H. Xu, J.Y. Chen, Y.N. Zhang, T. Liu, J.J. Fu, A fast room-temperature self-healing glassy polyurethane, Angew. Chem.-Int. Edit. 60 (2021) 7947–7955.
[26] R.C. Du, Z.C. Xu, C. Zhu, Y.W. Jiang, H.P. Yan, H.C. Wu, et al., A highly stretchable and self-healing supramolecular elastomer based on sliding crosslinks and hydrogen bonds, Adv. Funct. Mater. 30 (2020) 9.
[27] D.I. Lee, S.H. Kim, D.S. Lee, Synthesis of self-healing waterborne polyurethane systems chain extended with chitosan, Polymers 11 (2019) 11.
[28] H.C. Swart, J.J. Terblans, O.M. Ntwaeaborwa, R.E. Kroon, B.M. Mothudi, PL and CL degradation and characteristics of SrAl2O4: Eu2+,Dy3+ phosphors, Physica B 407 (2012) 1664–1667.
[29] W.X. Gao, W.Y. Ge, J.D. Shi, Y. Tian, J.F. Zhu, Y.X. Li, Stretchable, flexible, and transparent SrAl2O4:Eu2+@TPU ultraviolet stimulated anti-counterfeiting film, Chem. Eng. J. 405 (2021) 10.
[30] J.H. Kang, D. Son, G.J.N. Wang, Y.X. Liu, J. Lopez, Y. Kim, et al., Tough and water-insensitive self-healing elastomer for robust electronic skin, Adv. Mater. 30 (2018) 8.